Analyst

PAPER

View Article Online
View Journal | View Issue

Cite this: *Analyst*, 2014, **139**, 6197

Metal–organic frameworks and β-cyclodextrin-based composite electrode for simultaneous quantification of guanine and adenine in a lab-on-valve manifold†

Yang Wang,* Huanhuan Chen, Yichun Wu, Huali Ge, Guiqin Ye and Xiaoya Hu*

Received 19th May 2014
Accepted 9th September 2014

DOI: 10.1039/c4an00901k

www.rsc.org/analyst

In this work, a novel chemically modified electrode is constructed based on metal–organic frameworks and β-cyclodextrin ($Cu_3(BTC)_2$/β-CD, BTC = benzene-1,3,5-tricarboxylate) composite material. The electrode was used for simultaneous determination of guanine and adenine in a sequential injection lab-on-valve format and exhibited sensitive responses to guanine and adenine oxidation due to the π–π stacking interaction of $Cu_3(BTC)_2$ and the inclusion behavior of β-CD. The analytical performance was assessed with respect to the supporting electrolyte and its pH, accumulation time and accumulation potential, and the fluid flow rates. Under optimal conditions, linear calibration ranges for both guanine and adenine were from 1.0×10^{-7} to 1.0×10^{-5} mol L^{-1}, and detection limits ($S/N = 3$) were found to be 5.2×10^{-8} and 2.8×10^{-8} mol L^{-1}, respectively. The proposed sensor showed advantages of high sensitivity, simple sample preparation protocol, enhanced throughput and good reproducibility. Finally, the practical application of the proposed sensor has been performed for the determination of guanine and adenine in real samples with satisfactory results.

Introduction

Deoxyribonucleic acid (DNA) is composed of sugar phosphate backbone and nucleotide bases, which plays a crucial role in the storage unit for heredity information. The bases in DNA are adenine, guanine, cytosine and thymine. The abnormal changes of nucleic acid bases in the organism create defects and mutations of the immune system and may lead to various diseases.[1,2] Thus far, the principal strategies for the separation and quantification of bases in nucleic acids include high-performance liquid chromatography, micellar electrokinetic capillary chromatography with electrochemical detection and at-line SERS with high-performance liquid chromatography.[3–5] Owing to high sensitivity and selectivity, fast response, low cost and facile sample pre-treatment, various approaches have been utilized in the design of electrochemical sensors based on the electroactive nature of DNA bases. Advanced materials, such as functionalized grapheme,[6] carbon ionic liquid,[7] TiO_2 nanoparticles–magnesium(II)-doped natrolite zeolite,[8] graphitized mesoporous carbon,[9] graphene–ionic liquid–chitosan composite film,[10] cyclodextrin,[11] TiO_2–graphene nanocomposite,[12] CeO_2 nanoparticles decorated with multi-walled carbon nanotubes[13] and silver nanoparticles–polydopamine–graphene nanocomposite,[14] have been developed to produce modified electrodes to increase detection sensitivity for guanine and adenine detection.

As one of the most frequently investigated metal–organic frameworks, $Cu_3(BTC)_2$ (BTC = benzene-1,3,5-tricarboxylate) shows interesting properties in hydrogen, methane and carbon dioxide storage, gas separation and catalysis.[15–17] Moreover, $Cu_3(BTC)_2$ with large porosity and high surface area was also considered an ideal material in the fabrication of electrochemical sensors. For example, copper(II)-based metal–organic frameworks were used as selective electrocatalysts for the reduction of O_2 and CO_2.[18,19] Recent reports demonstrated that Au–SH–SiO_2 nanoparticles supported on metal–organic framework were utilized as sensors for electrocatalytic oxidation and determination of hydrazine and L-cysteine.[20,21] Our previous work also demonstrated that multi-walled carbon nanotubes and metal–organic framework composites can be used as novel electrode materials for lead sensors in environmental water samples.[22] CDs are cyclic oligosaccharides of a glucopyranose, containing a relatively hydrophobic central cavity and a hydrophilic outer surface. The parent or natural CD consists of 6, 7 or 8 glucopyranose units and is named α, β, or γ-CD, respectively. β-CD has been employed as a modifier in voltammetry for analysis of guest molecules by forming supramolecular complexes and thus enhancing sensitivity and selectivity for the analyte of interest.[23–27]

College of Chemistry and Chemical Engineering, Yangzhou University, Yangzhou 225002, China. E-mail: wangyzu@126.com; xyhu@yzu.edu.cn; Fax: +86 514 87975587; Tel: +86 514 87975587

† Electronic supplementary information (ESI) available. See DOI: 10.1039/c4an00901k

Currently, the combination of sequential injection lab-on-valve (SI-LOV) with electrochemical techniques has proved to be of great value and practical applicability.[28–30] This strategy offers many potential advantages, such as good reproducibility, less time consumption, and easy automation for high sample throughput. In the present work, a novel $Cu_3(BTC)_2$/β-CD modified electrode was fabricated, characterized and further applied to differential pulse voltammetric determination of guanine and adenine. The sensor combined the sequential injection lab-on-valve system to develop an automatic analytical procedure, and the feasibility of the proposed electrochemical sensor was demonstrated by applying it to the simultaneous determination of guanine and adenine in food and biological samples.

Experimental

Apparatus

Electrochemical measurements were performed with a CHI 852C electrochemical workstation (Shanghai Chenhua Instrument Company, China). A three-electrode system with a glassy carbon electrode (GCE) as the working electrode, an Ag/AgCl electrode as the reference electrode and a platinum wire as the auxiliary electrode, was employed in the measurements. Static contact-angle measurements were carried out at 20 °C with a sessile drop method using a CAM200 optical contact angle analyzer (KSV Instruments, Finland). The scanning electron micrograph (SEM) images were obtained with the Hitachi S-4800 (Japan). A FIAlab-3000 sequential injection system (FIAlab Instruments, Bellevue, WA, USA) equipped with a 2.5 mL syringe pump (Cavro, Sunnyvale, CA, USA) and a homemade LOV microconduit interfaced to match a six-port selection. All externally used tubes were made of 0.8 mm i.d. PTFE tubing (Upchurch Scientific, Oak Harbor, WA, USA).

Reagents and materials

Guanine and adenine 0.01 mol L^{-1} stock solutions were prepared by dissolving 0.1511 and 0.1351 g of guanine and adenine (Jinshan Chemicals, Shanghai, China) in 100 mL 0.05 mol L^{-1} sodium hydroxide. Working standard solutions were obtained by stepwise dilution. Copper nitrate trihydrate ($Cu(NO_3)_2 \cdot 3H_2O$), benzene-1,3,5-tricarboxylate (BTC), β-cyclodextrin, and *N*,*N*-dimethylformamide (DMF) used in this work were analytical grade, purchased from Sinopharm Chemical Reagent Co., Ltd (Shanghai, China). Phosphate buffer solution was prepared by mixing the stock solution of 0.1 mol L^{-1} NaH_2PO_4 and 0.1 mol L^{-1} Na_2HPO_4 and adjusting the pH at 7.0 with 0.1 mol L^{-1} H_3PO_4 or 0.1 mol L^{-1} NaOH solution. Double deionized water (18 MΩ cm) was prepared *via* the Milli-Q water purification system (Millipore, Bedford, MA, USA).

Synthesis of $Cu_3(BTC)_2$

$Cu_3(BTC)_2$ was prepared according to the following procedure after a minor modification.[31] First, 0.0945 g H_3BTC was dissolved in 6 mL ethanol, and 0.2178 g $Cu(NO_3)_2 \cdot 3H_2O$ was dissolved in 3 mL water. The two solutions were mixed and heated subsequently to 120 °C for 12 h. After the reaction, the blue crystals of $Cu_3(BTC)_2$ were isolated by filtration and washed with water. The product was dried at 100 °C for 8 h before use.

Fabrication of working electrode

One milligram of $Cu_3(BTC)_2$ and 10 mg β-CD were dispersed into 1.0 mL DMF by ultrasonic agitation for 2 h to give a homogeneous suspension. The glassy carbon electrode (3 mm in diameter) was polished successively with 1.0, 0.3, and 0.05 mm aluminum oxide powder on chamois leather. Then it was rinsed with doubly distilled water and sonicated in ethanol and doubly distilled water for 5 min. The electrode was immediately dried with highly purified nitrogen gas. After cleaning, the 5.0 μL suspension was placed on the cleaning glassy carbon electrode surface, and the solvent was allowed to evaporate under an infrared lamp. The obtained modified electrode was stored in air at room temperature.

Sample preparation

All samples were collected from the local supermarket or hospital. Beer and urine samples were degassed ultrasonically and further filtrated using 0.2 mm membrane filter before analysis. Two grams of beef were weighed and homogenized in 10 mL deionized water using mortar and pestle. After filtration, the extract was diluted to 100 mL with deionized water. The blood sample with EDTA as the anticoagulant was ultracentrifuged and the blood plasma obtained. Parts of the blood sample were diluted to 10 mL with deionized water for determination.

Operating procedure

The operation manifold was shown in Fig. 1, and the operating sequence was summarized from the following description: 500 μL carrier (deionized water) was drawn to clean all the lines and remove possible air bubbles *via* port 2. Then, 500 μL of air, 700 μL of phosphate buffer solution, 500 μL of sample, and 700 μL of phosphate buffer solution were sequentially aspirated into the holding coil *via* ports 5, 1 and 6, where the sample merged with the phosphate buffer solution; after flow reversal, the mixed sample/reagent zones were propelled

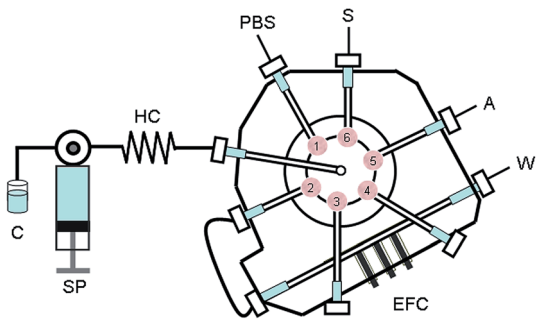

Fig. 1 Schematic diagram of the SI-LOV system in conjunction with voltammetry for simultaneous quantification of guanine and adenine. C: carrier (H_2O); SP: syringe pump; HC: holding coil; W: waste; A: air; S: sample; PBS: phosphate buffer solution (pH = 7.0); EFC: electrochemical flow cell.

forward through the electrochemical flow cell at a rate of 16 μL s^{-1} *via* port 2, during which the analyte was accumulated onto the surface of the modified electrode with an accumulation potential of −0.3 V; the oxidation current was recorded by differential pulse voltammetric measurements in the potential range from 0.1 to 1.3 V.

Results and discussion

Characterization

The static contact angle is commonly used to characterize the relative hydrophobicity/hydrophilicity of the modified electrode surface. As shown in Fig. 2, the $Cu_3(BTC)_2$/GCE has a relatively hydrophobic interface with a contact angle of about 72.7°. Meanwhile $Cu_3(BTC)_2$/β-CD/GCE became much more hydrophilic with a contact angle of 34.9°. This phenomenon suggests the high adsorbability of the $Cu_3(BTC)_2$/β-CD modified electrode surface to water due to introduction of β-CD hydrophilic groups. Fig. 3 shows the SEM micrographs of $Cu_3(BTC)_2$ and $Cu_3(BTC)_2$/β-CD composites. $Cu_3(BTC)_2$ appears to be micron-sized crystals with typical octahedral morphology. When β-CD and $Cu_3(BTC)_2$ were ultrasonically agitated together, the small sheets/layers of β-CD were observed, indicating that β-CD was well combined with $Cu_3(BTC)_2$.

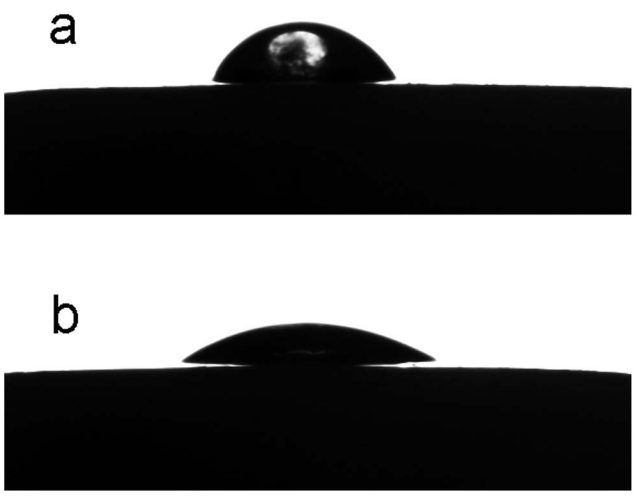

Fig. 2 Contact angle of water on $Cu_3(BTC)_2$/GCE (a), and $Cu_3(BTC)_2$/β-CD/GCE (b).

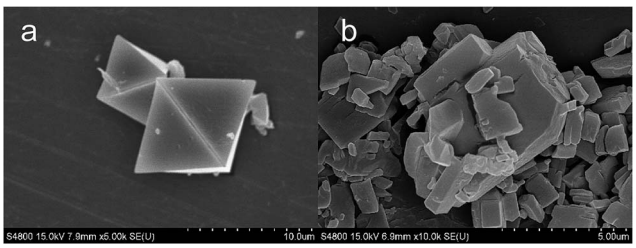

Fig. 3 SEM images of $Cu_3(BTC)_2$ (a) and $Cu_3(BTC)_2$/β-CD (b).

Electrochemical behaviors of guanine and adenine

The oxidation of these two bases using $Cu_3(BTC)_2$/β-CD/GCE by the differential pulse voltammetry experiments is investigated with a mixture of guanine and adenine in pH 7.0 phosphate buffer solution (Fig. 4). There were no oxidation peaks in the absence of guanine and adenine over the potential range from 0.3 to 1.3 V, indicating that all the electrodes were non-electroactive in the selected potential range. At the bare GCE, two small oxidation peaks were observed for guanine and adenine, indicating the sluggish electron transfer kinetics of guanine and adenine. In cases of the $Cu_3(BTC)_2$-modified electrode (curve b), two anodic peaks are observed with relatively larger peak currents. However, the reversible redox responses of Cu(II)/Cu(I) and Cu(0) to Cu(I) for $Cu_3(BTC)_2$ were not observed due to the different potential scan range.[19] $Cu_3(BTC)_2$ consists of metal ions and organic ligands and has the ability to interact with components through π–π stacking interactions. Both guanine and adenine have three aromatic rings. Hence, they may be adsorbed to the $Cu_3(BTC)_2$ surface through π–π stacking between the aromatic rings and the organic ligands.[32,33] After modification with β-CD, two well-defined oxidation peaks were observed with larger peak separations and higher peak currents corresponding to the oxidation of guanine and adenine, respectively. This can be attributed to the fact that with a hydrophobic inner cavity and a hydrophilic outer side, β-CD can be viewed as biological guest molecular receptors by forming stable host–guest inclusion complexes. At the $Cu_3(BTC)_2$/β-CD modified electrode, a substantial enhancement of guanine and adenine peaks is observed, due to the synergistic effect of the two kinds of functional materials. These results indicated that the $Cu_3(BTC)_2$/β-CD composite-modified electrode cannot only identify the guanine and adenine, but also enhance detection sensitivity. In addition, the peak-to-peak separation of guanine and adenine was 0.32 V, which was large enough to determine guanine and adenine simultaneously and effectively decrease the interaction between guanine and adenine.

Electrochemical mechanisms usually can be acquired from the relationship between peak current and scan rate. The cyclic voltammograms of $Cu_3(BTC)_2$/β-CD/GCE in phosphate buffer

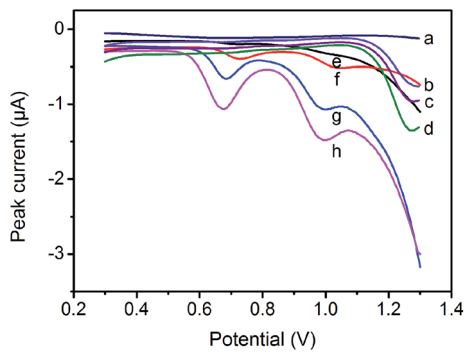

Fig. 4 Differential pulse voltammograms at bare GCE (a and e), $Cu_3(BTC)_2$/GCE (b and f), β-CD/GCE (c and g), $Cu_3(BTC)_2$/β-CD/GCE (b and h) in the absence (a–d) and presence of 10 μmol L^{-1} guanine and 10 μmol L^{-1} adenine (e–h) in pH 7.0 PBS.

solution at different scan rates were investigated in the range of 50–250 mV s^{-1}. Peak currents of the $Cu_3(BTC)_2$/β-CD/GCE increased with the increment of the scan rate. A good linear relationship could be observed between the peak current and scan rate in the range of 10–240 mV s^{-1} (Fig. S1†). For 0.5 μmol L^{-1} of guanine, the anodic peak followed the linear regression equation I_{pa} (μA) = 0.0181ν (mV s^{-1}) + 1.27 (R^2 = 0.9912). For 0.5 μmol L^{-1} of adenine, the regression equation was I_{pa} (μA) = 0.00557ν (mV s^{-1}) + 0.446 (R^2 = 0.9920). These results indicated that the electrode reaction of guanine and adenine at $Cu_3(BTC)_2$/β-CD/GCE was a typical adsorption-controlled process.

Effects of supporting electrolyte and its pH

Different supporting electrolytes including sulfuric acid, acetic acid, phosphate buffer solution, Britton–Robinson buffer solution and acetate buffer solution were studied in order to find the appropriate medium for oxidation of guanine and adenine. The phosphate buffer solution gives the best stripping peak shape and the highest stripping peak current. Therefore, phosphate buffer solution was chosen as the determining medium. Another parameter affecting the electrochemical response of the $Cu_3(BTC)_2$/β-CD/GCE is the pH of the supporting electrolyte. Variations of peak current with respect to pH of the electrolyte in the range of 5.0–9.0 were investigated (Fig. S2†). The anodic peak currents of guanine and adenine increase slightly with increasing pH from 5.0 to 7.0. This phenomenon can be attributed to the fact that biochemical compounds are more stable in pH = 7 solution. However, peak currents decrease as pH increases further, because the increase of OH^- will lead to the reduction of protons, resulting in the slowdown of the chemical oxidation process. Therefore, a 0.1 mol L^{-1} phosphate buffer solution with pH 7.0 was selected. In addition, all anodic peak currents for oxidation of guanine and adenine shifted towards more negative potential with an increase in pH, showing that protons have taken part in their electrode reaction processes. Linear relationships of the peak potential of DNA bases and the pH were $E_{pa,\ guanine}$ = −0.058 pH + 1.116, R^2 = 0.9923; $E_{pa,\ adenine}$ = −0.063 pH + 1.461, R^2 = 0.9906 with slopes of 58 and 63 mV per pH, respectively. These results were close to the expected Nernstian theoretical value of 58 mV per pH at 25 °C, suggesting that the electron uptake was accompanied by an equal number of protons. This conclusion is in accordance with the known two electrons/two protons electrochemical reactions of guanine and adenine,[8,12] and the oxidation mechanism of guanine and adenine was shown in Fig. S3.†

Effects of accumulation potential and accumulation time

The effect of accumulation potential on the anodic peak currents of guanine and adenine solutions was examined over the −0.1 to −0.5 V range (Fig. S4†). The peak current of guanine initially increased, obviously by changing accumulation potential from −0.1 to −0.3 V and then rapidly decreased from −0.3 to −0.5 V. At the same time, the peak current of adenine increased slightly with increase of potential from −0.1 to −0.3 V and decreased above −0.3 V. Thus the accumulation potential of −0.3 V was chosen as the optimum accumulation potential for further experiments. The peak current increased with deposition time increasing up to 180 s (Fig. S5†), and no saturated adsorption of guanine and adenine at the electrode surface was observed. Considering both high sensitivity and short analysis time, the optimal accumulation time of 120 s was employed in further experiments.

Effect of sample solution flow rate

In a flow system, sample flow rate has a significant effect on the adsorption of analyte when passing through the electrochemical flow cell, which was thus investigated within a range of 8–24 μL s^{-1} (Fig. S6†). The signal intensities of guanine and adenine gradually increased with the flow rate until 16 μL s^{-1} and then decreased at a higher sample flow rate. The phenomenon indicated that the adsorption process of guanine and adenine on the electrode surface was not instantaneously achieved. A higher flow rate was facilitated to improve the signal intensity by less dispersion between bases and the electrode surface. However, an excessively high flow rate could seriously deteriorate the $Cu_3(BTC)_2$/β-CD modifier on the electrode surface. As a compromise, a sample flow rate of 16 μL s^{-1} was finally used throughout this work.

Study of interferences

Possible interferences for the detection of guanine and adenine in food and biological samples were investigated by adding various foreign species into the phosphate buffer solution containing 0.5 μmol L^{-1} guanine and 0.5 μmol L^{-1} adenine. The tolerance limit was defined as the maximum concentration of the interference substances that brought less than ±5% relative error in the detection. It was found that 500-fold of glucose, cysteine, glycine, glutamic acid, lactic acid, deoxyribose, ribose, cholesterin, uric acid, thymine, and ascorbic acid had no significant interference. Xanthine and hypoxanthine were also studied, because their structures were very similar to the target analytes. The results indicated that 30-fold of xanthine and hypoxanthine can influence the peak potential and current response of adenine. Furthermore, the common inorganic ions such as Na^+, K^+, Ca^{2+}, Fe^{3+}, Cu^{2+}, NO_3^-, and SO_4^{2-} had almost no interference on the determination (at least 10 000-fold). Therefore, the modified electrode can be considered a good electrochemical sensor for recognition of guanine and adenine.

Individual determination of guanine and adenine

Under optimized conditions, differential pulse voltammograms are recorded for the individual determination of guanine and adenine in phosphate buffer solution (pH 7.0) at a scan rate of 50 mV s^{-1}. The voltammetric responses of different concentrations of guanine and adenine were evaluated when the concentration of one changed, whereas the other was kept constant. Fig. 5 shows that the anodic peak current for guanine increased with higher guanine concentration in the ranges 0.1–1 μmol L^{-1} and 1–10 μmol L^{-1}, while the response current of adenine was kept constant (0.3 μmol L^{-1}). Similarly, the influence of adenine concentration was checked by increasing the

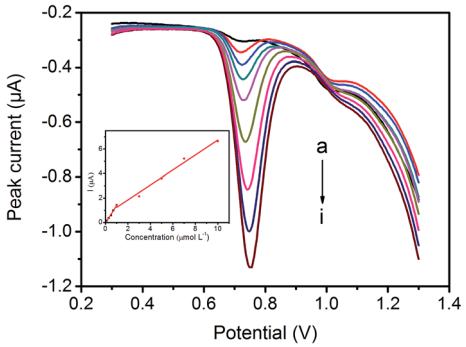

Fig. 5 Differential pulse voltammograms of different concentrations of guanine in the presence of 0.3 μmol L^{-1} of adenine at $Cu_3(BTC)_2$/β-CD/GCE. Guanine concentrations: (a) 0.1, (b) 0.3, (c) 0.5, (d) 0.7, (e) 1, (f) 3, (g) 5, (h) 7 and (i) 10 μmol L^{-1}. Optimized instrument parameters: pulse width 0.2 s, pulse period 0.5 s, and step increment 4 mV. Inset: linear range of peak current *versus* concentration of guanine.

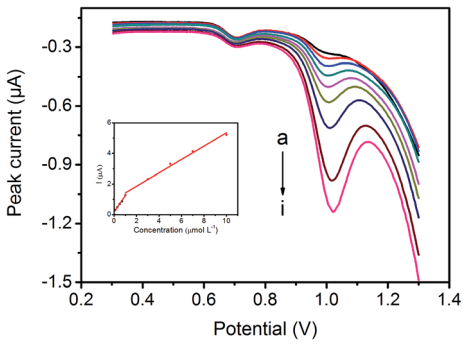

Fig. 6 Differential pulse voltammograms of different concentrations of adenine in presence of 0.3 μmol L^{-1} of guanine at $Cu_3(BTC)_2$/β-CD/GCE. Adenine concentrations: (a) 0.1, (b) 0.3, (c) 0.5, (d) 0.7, (e) 1, (f) 3, (g) 5, (h) 7 and (i) 10 μmol L^{-1}. Optimized instrument parameters: pulse width 0.2 s, pulse period 0.5 s and step increment 4 mV. Inset: linear range of peak current *versus* concentration of adenine.

adenine concentration while keeping the guanine concentration constant at 0.3 μmol L^{-1}. As shown in Fig. 6, the anodic peak current for adenine was directly proportional to its concentration in the ranges 0.1–1 μmol L^{-1} and 1–10 μmol L^{-1}, while the peak currents related to the guanine did not obviously change. Hence the change in concentration of one studied base did not have a significant influence on the other one. The calibration graphs of the two bases had two linear sections, and the first had a higher slope than the second. This phenomenon could be ascribed to the fact that the absorption process at the modified electrode surface is predominant at the low concentration range and the diffusion process on the monolayer-covered surface occurred at the high concentration range. Similar results have been reported for guanine and adenine quantification.[12,34,35]

Simultaneous determination of guanine and adenine

To investigate the potential of the $Cu_3(BTC)_2$/β-CD-modified electrode for simultaneous determination of guanine and adenine, the peak current responses of these species when

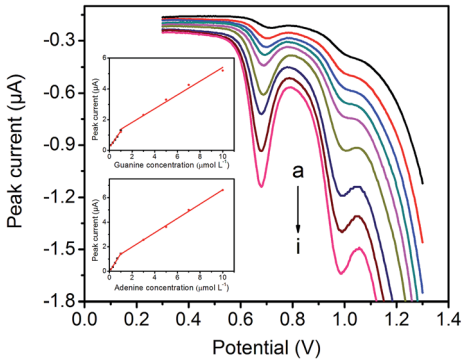

Fig. 7 Differential pulse voltammograms of mixture solution containing guanine and adenine at equal concentrations in phosphate buffer (pH = 7.0) at $Cu_3(BTC)_2$/β-CD/GCE: (a) 0.1, (b) 0.3, (c) 0.5, (d) 0.7, (e) 1, (f) 3, (g) 5, (h) 7 and (i) 10 μmol L^{-1}. Optimized instrument parameters: pulse width 0.2 s, pulse period 0.5 s and step increment 4 mV. Inset: dependencies between peak current (μA) and bases concentration (μmol L^{-1}).

simultaneously changing concentrations of guanine and adenine in a mixture were measured by differential pulse voltammetry. As shown in Fig. 7, the $Cu_3(BTC)_2$/β-CD-modified electrode exhibited two well-defined and distinguishable anodic peaks for the oxidation of guanine and adenine, which matches well with their individual anodic peak potential as discussed in the above section. It can also be observed that the peak currents of both bases increased linearly with their concentrations, and both oxidation peaks were well separated on the $Cu_3(BTC)_2$/β-CD-modified electrode without interfering with each other. Linear equations and detection limits are listed in Table 1. The limit of detection was calculated by IUPAC, defined as LOD = $3\sigma/s$, where σ is the standard deviation of the blank signals and s is the slope of the linear calibration graph. A relative standard deviation (R.S.D.) of 2.52% and 3.03% for 10 measurements of 0.5 μmol L^{-1} of guanine and adenine mixture suggested that $Cu_3(BTC)_2$/β-CD/GCE had good repeatability. Comparing the data showed that improved performance for the simultaneous determination of guanine and adenine can be achieved using the $Cu_3(BTC)_2$/β-CD/GCE, as displayed in Table 2. The analytical parameters including detection limit and linear range are better or comparable to other reports using different modified electrode materials. Thus, $Cu_3(BTC)_2$/β-CD/GCE is a promising candidate for construction of sensitive and selective biosensors. More importantly, the $Cu_3(BTC)_2$/β-CD-modified electrode is applicable to the sequential injection LOV system. The combined techniques offer advantages in comparison to the traditional batch voltammetric methods, such as reduced sample/reagent consumption, programmable flow and outline means for miniaturization of assays. The long-term stability of $Cu_3(BTC)_2$/β-CD/GCE was further studied within the LOV and then the anodic peak currents were recorded. The results indicated that current response remained unchanged after continuous scanning for 15 cycles, indicating that the $Cu_3(BTC)_2$/β-CD/GCE was stable in the on-line flow system.

Table 1 Simultaneous determination of guanine and adenine at $Cu_3(BTC)_2$/β-CD/GCE

DNA bases	Linear range (μmol L^{-1})	Linear equation (μA, μmol L^{-1})	R^2	Detection limit (μmol L^{-1})
Guanine	0.1–1	$I_{pa} = 1.476C - 0.0435$	0.9966	0.052
	1–10	$I_{pa} = 0.582C + 0.813$	0.9992	
Adenine	0.1–1	$I_{pa} = 1.072C + 0.186$	0.9939	0.028
	1–10	$I_{pa} = 0.448C + 0.925$	0.9938	

Table 2 Comparison of proposed method with selected previously reported electrochemical methods for determination of guanine and adenine[a]

		Linear range (μmol L^{-1})		Detection limit (μmol L^{-1})			
Methods	Technique	Guanine	Adenine	Guanine	Adenine	System	Ref.
G–COOH/GCE	DPV	0.5–200		0.05	0.025	Batch	6
CILE/CPE	CV	0.3–50	1.5–70	0.0787	0.25	Batch	7
TiO_2NPs–MgY/ZMCPE	DPV	0.1–10		0.013	0.02	Batch	8
GMC/GCE	DPV	25–200	25–150	0.76	0.63	Batch	9
GS–IL–CS/GCE	DPV	2.5–150	1.5–350	0.75	0.45	Batch	10
PNAANI/CPE	DPV	0.1–10		0.05		Batch	11
TiO_2–G/GCE	DPV	0.5–200		0.15	0.1	Batch	12
CeO_2–MWCNTs/GCE	DPV	5–50	5–35	0.01	0.02	Batch	13
$Cu_3(BTC)_2$/β-CD/GCE	DPV	0.1–10		0.052	0.028	Automatic	This work

[a] G–COOH: graphene–COOH; CILE: carbon ionic liquid electrode; TiO_2NPs–MgY/ZMCPE: TiO_2 nanoparticles–magnesium-doped zeolite Y-modified carbon paste electrode; GMC: graphitized mesoporous carbon; GS–IL–CS: graphene sheets–ionic liquid–chitosan; PNAANI: cyclodextrin-modified poly(*N*-acetylaniline); TiO_2–G: TiO2–graphene; CeO_2–MWCNTs: CeO_2 nanoparticles decorated multi-walled carbon nanotubes; GCE: glassy carbon electrode; CPE: carbon paste electrode; DPV: differential pulse voltammetry; CV: cyclic voltammetry.

Table 3 Determination of guanine and adenine in food and biological samples

Sample	Analyte	Original (μmol L^{-1})	Added (μmol L^{-1})	Found (μmol L^{-1})	Recovery (%)
Beef	Guanine	6.54	4	10.51	99.2
	Adenine	6.02	4	10.06	101
Beer	Guanine	3.70	4	7.80	102.5
	Adenine	1.02	4	4.97	98.7
Blood	Guanine	—	0.5	0.49	98.0
			5	4.98	99.6
	Adenine	—	0.5	0.48	96.0
			5	5.05	101.0
Urine	Guanine	—	0.5	0.48	96.0
			5	4.93	98.6
	Adenine	—	0.5	0.51	102.0
			5	4.89	97.8

Analytical applications

In order to ascertain its potential application, the utilization of the $Cu_3(BTC)_2$/β-CD/GCE in real samples was investigated by analysis of guanine and adenine in food and biological samples. For the sample analyses, 500 μL of sample solution was taken and recovery experiments were performed by measuring the differential pulse voltammetry responses, in which known concentrations of guanine and adenine were added. High recoveries were achieved at a range of 96.0–102.5% for all the samples (Table 3), suggesting that the proposed method is feasible and effective with high accuracy.

Conclusion

In this work, we have successfully developed an electrochemical method for simultaneous determination of guanine and adenine at the $Cu_3(BTC)_2$/β-CD/GCE in a miniaturized and automatic sequential injection LOV system. Well-defined peaks and significant increase of peak currents were observed by adsorption of guanine and adenine compounds at the $Cu_3(BTC)_2$/β-CD/GCE surface, which clearly demonstrated that the composite material could be used as an efficient promoter to enhance kinetics of the electrochemical process of guanine

and adenine. The effects of potential interfering species were studied, and it was found that the proposed procedure was free from interferences of most common interfering ions and organic compounds. The proposed sensor was employed in determination of guanine and adenine in food and biological samples with satisfactory recovery. Thus, our proposed method might be adopted as an alternative method for quantitative determination of electroactive biomolecules with high sensitivity and speed.

Acknowledgements

This work was supported by the National Natural Science Foundation of China (21205103, 21275124), Jiangsu Province Nature Foundation of China (BK2012258), and the Priority Academic Program Development of Jiangsu Higher Education Institutions.

References

1 J. D. Carver and W. Allan Walker, *J. Nutr. Biochem.*, 1995, **6**, 58–72.
2 K. Sandoval Guerrero, A. Revilla Vázquez, B. Segura-Pacheco and A. Dueñas-Gonzalez, *Electrophoresis*, 2005, **26**, 1057–1062.
3 T. Fukuuchi, M. Yasuda, K. Inazawa, T. Ota, N. Yamaoka, K. Mawatari, K. Nakagomi and K. Kaneko, *Anal. Sci.*, 2013, **29**, 511–517.
4 G. Chen, X. Han, L. Zhang and J. Ye, *J. Chromatogr. A*, 2002, **954**, 267–276.
5 C. Carrillo-Carrión, S. Armenta, B. M. Simonet, M. Valcárcel and B. Lendl, *Anal. Chem.*, 2011, **83**, 9391–9398.
6 K. J. Huang, D. J. Niu, J. Y. Sun, C. H. Han, Z. W. Wu, Y. L. Li and X. Q. Xiong, *Colloids Surf., B*, 2011, **82**, 543–549.
7 W. Sun, Y. Z. Li, Y. Y. Duan and K. Jiao, *Biosens. Bioelectron.*, 2008, **24**, 988–993.
8 M. Arvand, R. Motaghed Mazhabi and A. Niazi, *Electrochim. Acta*, 2013, **89**, 669–679.
9 R. Thangaraj and A. Senthil Kumar, *J. Solid State Electrochem.*, 2013, **17**, 583–590.
10 X. Niu, W. Yang, J. Ren, H. Guo, S. Long, J. Chen and J. Gao, *Electrochim. Acta*, 2012, **80**, 346–353.
11 A. Abbaspour and A. Noori, *Analyst*, 2008, **133**, 1664–1672.
12 Y. Fan, K. J. Huang, D. J. Niu, C. P. Yang and Q. S. Jing, *Electrochim. Acta*, 2011, **56**, 4685–4690.
13 Y. Wei, Q. A. Huang, M. G. Li, X. J. Huang, B. Fang and L. Wang, *Electrochim. Acta*, 2011, **56**, 8571–8575.
14 K. J. Huang, L. Wang, H. B. Wang, T. Gan, Y. Y. Wu, J. Li and Y. M. Liu, *Talanta*, 2013, **114**, 43–48.
15 N. C. Jeong, B. Samanta, C. Y. Lee, O. K. Farha and J. T. Hupp, *J. Am. Chem. Soc.*, 2011, **134**, 51–54.
16 J. L. C. Rowsell and O. M. Yaghi, *J. Am. Chem. Soc.*, 2006, **128**, 1304–1315.
17 K. Schlichte, T. Kratzke and S. Kaskel, *Microporous Mesoporous Mater.*, 2004, **73**, 81–88.
18 J. Mao, L. Yang, P. Yu, X. Wei and L. Mao, *Electrochem. Commun.*, 2012, **19**, 29–31.
19 R. Senthil Kumar, S. Senthil Kumar and M. Anbu Kulandainathan, *Electrochem. Commun.*, 2012, **25**, 70–73.
20 H. Hosseini, H. Ahmar, A. Dehghani, A. Bagheri, A. R. Fakhari and M. M. Amini, *Electrochim. Acta*, 2013, **88**, 301–309.
21 H. Hosseini, H. Ahmar, A. Dehghani, A. Bagheri, A. Tadjarodi and A. R. Fakhari, *Biosens. Bioelectron.*, 2013, **42**, 426–429.
22 Y. Wang, Y. C. Wu, J. Xie, H. L. Ge and X. Y. Hu, *Analyst*, 2013, **138**, 5113–5120.
23 U. Yogeswaran, S. Thiagarajan and S. M. Chen, *Carbon*, 2007, **45**, 2783–2796.
24 A. Abbaspour and A. Noori, *Analyst*, 2012, **137**, 1860–1865.
25 Z. H. Wang, S. F. Xiao and Y. Chen, *J. Electroanal. Chem.*, 2006, **589**, 237–242.
26 Z. H. Wang, S. F. Xiao and Y. Chen, *Electroanalysis*, 2005, **17**, 2057–2061.
27 Q. Shen and X. Wang, *J. Electroanal. Chem.*, 2009, **632**, 149–153.
28 I. Lahdesmaki, Y. K. Park, A. D. Carroll, M. Decuir and J. Ruzicka, *Analyst*, 2007, **132**, 811–817.
29 J. Jakmunee, L. Patimapornlert, S. Suteerapataranon, N. Lenghor and K. Grudpan, *Talanta*, 2005, **65**, 789–793.
30 Y. Wang, Z. Liu, G. Yao, P. Zhu, X. Hu, C. Yang and Q. Xu, *Anal. Chim. Acta*, 2009, **649**, 75–79.
31 K. Peikert, F. Hoffmann and M. Fröba, *Chem. Commun.*, 2012, **48**, 11196–11198.
32 C. X. Yang and X. P. Yan, *Anal. Chem.*, 2011, **83**, 7144–7150.
33 Y. Y. Fu, C. X. Yang and X. P. Yan, *J. Chromatogr. A*, 2013, **1274**, 137–144.
34 J. M. Zen, M. R. Chang and G. Ilangovan, *Analyst*, 1999, **124**, 679–684.
35 H. S. Wang, H. X. Ju and H. Y. Chen, *Anal. Chim. Acta*, 2002, **461**, 243–250.